Optimal Allocation of Wind and Solar Based Distributed Generation in a Radial Distribution System

Kola Sampangi Sambaiah[*], T Jayabarathi[**‡]

*School of Electrical Engineering, Research Scholar, VIT University, Vellore.

** School of Electrical Engineering, Senior Professor, VIT University, Vellore.

(sampangi.sambaiah@vit.ac.in, tjayabarathi@vit.ac.in)

[‡]T. Jayabarathi; VIT University, Vellore, India, Tel: +0416 224 2891, Fax: +0416 224 3092, tjayabarathi@vit.ac.in

Received: 08.09.2018 Accepted:30.10.2018

Abstract- Decentralized power generation from renewable energy sources (RES) is a long-term solution that addresses present environmental threats because of its widespread availability, sustainability, nonpolluting generation and eco-friendliness. The most widely used renewable distributed generation (RDG) are wind turbine (WT) and solar photovoltaic (PV) systems. But power generated from WT and solar PV systems is intermittent. Since wind speed and solar irradiance have random nonlinear generation patterns a suitable probabilistic method is adopted to model these uncertainties. A new hybrid grey wolf optimizer (HGWO) algorithm is proposed for optimal allocation of WT and solar PV systems in a distribution network considering the following constraints: discrete DG size limits, DG penetration limits, line loading capacity and bus voltage stability limits. The proposed method is tested on a 28-bus Indian distribution network which is located in Kakdwip, India. The results obtained by the proposed HGWO algorithm are presented and compared with the existing particle swarm optimization (PSO) algorithm and found to be better.

Keywords Renewable Energy Source, Optimal DG Allocation, Metaheuristic Optimization, Hybrid Grey Wolf Optimizer, Wind and Solar DG, Renewable Distributed Generation.

1. Introduction

Electricity is considered as the foremost important source for a country's economic growth. Centralized power generating stations are the primary source of electricity. These generating stations mainly depend on fossil fuels for power generation. Large utilization of fossil fuels causes global warming and resource depletion. In the near future, one of the major challenges is to achieve clean, safe and sustainable power generation using RES to supply the growing power demand [1].

The energy crisis of the 1970s enlightens many researchers and the world society for making a changeover to an alternative power generation through RES like wind and solar. However, many countries adopt strict environmental and sustainable policies for encouraging generation through RES. These policies make RES based distributed generation (DG) as a paramount alternative for distribution network operators [2,3]. But, penetration of RDG leads to various challenges because of uncertainty in power generation [4].

However, power generation by WTs and solar PV system for a particular region is almost complimentary because wind speed is high during night and solar irradiance is high during day. This optimum mixture will give maximum potential benefits.

Strategic allocation and operation of these DGs in a network defer major system upgrades, diminish distribution network power loss, enhance voltage profile and extend the equipment reliability by relieving the heavily loaded feeders [5]. Appropriate allocation and sizing of WT and solar PV system are vital in a distribution network's performance since inappropriate allocation leads to adverse effects [6,7,36].

In last few years several researchers have made a significant contribution to RES planning. A combination or a mix of two or more RES allocation and sizing is known as hybrid system planning problems. In the past several deterministic approaches have been used for solving these problems. However, in recent years, various heuristic or meta-heuristic optimization algorithms are found to be performing well for solving these problems.

In [8] an analytical method is utilized for sizing a hybrid solar-wind (HSW) based standalone system appropriately with accounting the level of autonomy by the time division for limited supply load and system cost.

An HSW sizing technique was proposed to optimize the hybrid system, power loss probability, and levelised energy cost in [9]. A deterministic method is proposed for optimal sizing and evaluating energy cost of the renewable hybrid system by incorporating probabilistic power generation in [10]. A heuristic optimization technique is proposed in [11] for autonomous HSW system design along with battery storage. A genetic algorithm is used to assess an optimal number of units and type of PV modules, WTs and batteries by covering complete load with zero load rejection for 20-years operation period. In [12] simulated annealing is used in the optimal sizing of HSW system with battery storage keeping annualized system cost as the objective.

In literature most of the studies concentrated on standalone HSW system and a few studies investigated the grid integrated hybrid energy system. In [13], the authors comprehensively explained how the grid performance is affected by integrating RES into the grid and significant relationship between the power demand and RES generation models are considered. Thereby substantial reduction in grid dependency and minimization of network power loss through integrating renewable DGs into the grid. In [14], an evolutionary programming-based optimization method is utilized for optimal allocation of RDGs in a radial distribution system (RDS) by considering annual energy loss minimization as objective. Advantages of renewable energy resources and modeling techniques have been presented in [28 – 35]. In [15] PSO algorithm is used for optimal allocation of solar, wind and mixed wind-solar DGs in RDS.

The HGWO algorithm has so far been used for solving economic dispatch problem in [16] and optimal DG allocation problem in [17]. In the present paper, the HGWO algorithm is used for optimal allocation and sizing of RDG in a radial distribution system. The power generation patterns of WT and solar PV system are evaluated using probabilistic studies. However, the proposed method possesses substantial reduction in power loss, grid dependency, and thereby improves bus voltage stability.

2. Probabilistic Models of Solar and Wind Power Generation

Power generation from solar and wind systems purely depends on meteorological conditions like solar irradiance, ambient temperature and wind speed which are directly associated with the site. So, primary analysis of solar irradiance and wind speed characteristics at the installed site plays a vital role in utilizing WTs and PV systems efficiently [24].

2.1. RES model

The stochastic behavior of solar irradiance and wind speed can be analyzed in a statistical manner by probability distribution function (PDF).

2.1.1. Wind speed modeling

Weibull PDF is considered as a very good expression for modeling the wind speed behavior [18,19]. Weibull distribution of wind speed v^{tm} (m/s) at a particular time tm is expressed as

$$f_v^{tm}(v) = \frac{k^{tm}}{c^{tm}}\left(\frac{v^{tm}}{c^{tm}}\right)^{k^{tm}-1} * exp\left(-\left(\frac{v^{tm}}{c^{tm}}\right)^{k^{tm}-1}\right) \quad (1)$$

The scale factor (c^{tm}) and shape parameter (k^{tm}) at the time tm are evaluated using the following expressions

$$k^{tm} = \left(\frac{\sigma_v^{tm}}{\mu_v^{tm}}\right)^{-1.086} \quad (2)$$

$$c^{tm} = \frac{\mu_v^{tm}}{\Gamma\left(1+\frac{1}{k^{tm}}\right)} \quad (3)$$

where μ_v^{tm} and σ_v^{tm} are mean and standard deviation of wind speed at the time tm and Γ represents the gamma function.

2.1.2. Solar irradiance modeling

In general, solar irradiance imitates Beta PDF [18]. Beta distribution of solar irradiance s^{tm} at a particular time tm is expressed as

$$f_s^{tm}(s) = \frac{\Gamma(\alpha^{tm}+\beta^{tm})}{\Gamma(\alpha^{tm})*\Gamma(\beta^{tm})}(s^{tm})^{\alpha^{tm}-1} * (1-s^{tm})^{\beta^{tm}-1} \quad (4)$$

where α^{tm} and β^{tm} are the shape parameters at tm.

These shape parameters are evaluated by the known mean (μ_s^{tm}) and the standard deviation (σ_s^{tm}) of solar irradiance at a particular time tm as

$$\beta^{tm} = (1-\mu_s^{tm}) * \left(\frac{\mu_s^{tm}*(1+\mu_s^{tm})}{(\sigma_s^{tm})^2} - 1\right) \quad (5)$$

$$\alpha^{tm} = \frac{\mu_s^{tm}*\beta^{tm}}{(1-\mu_s^{tm})} \quad (6)$$

2.2. Wind and solar power generation models

The output powers of RDGs are calculated using continuous PDF. This continuous PDF with specific limits for solar irradiance and wind speed has been divided into several states (periods or intervals). Selecting a number of states is precisely taken for Weibull and Beta distribution, since these states affect solution accuracy.

2.2.1. Calculation of the PV system power generation

The PV system output power depends on PV module characteristics, ambient temperature, and irradiance of the location. Therefore, when Beta PDF is generated for a particular time tm, during different states the power output is evaluated at a particular time is P_{PV}^{tm} as follows

$$P_{PV}^{tm} = \sum_{\square=1}^{N_{ds}} PG_{PV\square}\left(s_{avg}\right) * P_s(s_{\square}^{tm}) \quad (7)$$

where stands for the state variable and $N_{ds}$is the discrete number of solar irradiance state. $s_{}^{tm}$is the ^{t}state of solar irradiance at the time tm.

The solar irradiance for each state with probability through any definite time interval (hour) is evaluated as

$$P_s(s_h^{tm}) = \int_{sh1}^{sh2} f_s^{tm}(s).ds \quad (8)$$

where $s1$and $s2$are solar irradiance limits of the state.

The average irradiance $(s_{avg})$of PV system output power for the state is evaluated as

$$PG_{PVh}(s_{avg}) = Nh_{h\,PVmod} \quad (9)$$

where $N_{PVmod}$is the sum of PV modules in an array; the following equations give the current-voltage (I-V) characteristic of a single PV module with respect to irradiance and ambient temperatureT_A (C) are

$$I_h = s_{avg}[I_{sc} + K_i(T_{ch} - 25)] \quad (10)$$

$$V_h = V_{oc} - K_v * T_{ch} \quad (11)$$

$$T_{ch} = T_A + s_{avg}\left(\frac{N_{OT}-20}{0.8}\right) \quad (12)$$

$$FF = \frac{V_{mpp}*I_{mpp}}{V_{oc}*I_{sc}} \quad (13)$$

$T_{c}$is cell temperature at ^{t}state (C); $K_i$and $K_v$are temperature coefficient of current (A/C) and voltage (V/C);$N_{OT}$is the cell nominal operating temperature (C);$V_{oc}$is open circuit voltage (V); $FF$is the fill factor;$I_{sc}$is short circuit current (A); $V_{mpp}$and $I_{mpp}$are maximum power point voltage (V) and current (A).

2.2.2. Calculation of the WT power generation

The wind turbine output depends on wind speed at the site as well as performance curve. Therefore, when Weibull PDF is generated for a particular timetm, during different states the power output is evaluated for the particular timeP_{WT}^{tm}as follows

$$P_{WT}^{tm} = \sum_{h=1}^{N_{ds}} PG_{WTh}\left(v_{avg}\right) * P_v(v_h^{tm}) \quad (14)$$

The wind speed for each state with probability over any definite time interval (hour) is evaluated as

$$P_v(v_h^{tm}) = \int_{vh1}^{vh2} f_v^{tm}(v).dv \quad (15)$$

where $v1$and $v2$are wind speed limits of the state.

The average wind speed$(v_{avg})$of WT output power for the state is evaluated as

$$PG_{WT}(v_{avg}) = \begin{cases} 0 \\ (a * v_{avg}^3 + b * P_{rated}) \\ P_{rated} \end{cases}$$

$$v_{cin} < v_{avg} \quad or \quad v_{avg} > v_{cout}$$

$$v_{cin} \le v_{avg} \le v_N$$

$$v_N \le v_{avg} \le v_{cout} \quad (16)$$

where $P_{rated}$is WT maximum or rated power; v_{cin},$v_N$and $v_{cout}$are cut-in, nominal and cut-out wind speeds; $a$and $b$are constants obtained as

$$a = \left(\frac{P_{rated}}{v_N^3 - v_{cin}^3}\right) \quad (17)$$

$$b = \left(\frac{v_{cin}^3}{v_N^3 - v_{cin}^3}\right) \quad (18)$$

3. Problem Formulation

The present objective is to ease distribution network with the mixed wind-solar system. It is significant to assess the technical consequences of new facilities on the network. It prevents power quality and reliability degradation. However, various technical issues are colligated with DG penetration into a distribution network. The major technical issues which are considered in the present study are network power loss, bus voltage stability and line loading capacity [20].

3.1. Objective function

In general, to lessen protection complication in a distribution network they are structured radially. RDS has high resistance to reactance ratio (R/X) causes high active power loss. It is very important to assess and reduce active power losses for increasing system operational efficacy. The primary objective of the present problem is power loss minimization and evaluating the corresponding voltage stability factor and network security index. The average power loss of the network per annum can be realized as

$$Ploss_{a,avg} = \frac{\sum_{tm=1}^{N_{tm}} \sum_{k=1}^{N_{ln}} \frac{r_k\left(\left(P_{D,k+1}^{tm}\right)^2 + \left(Q_{D,k+1}^{tm}\right)^2\right)}{\left(V_{k+1}^{tm}\right)^2}}{N_{tm}} \quad (19)$$

where $P_{D,k+1}^{tm}$and $Q_{D,k+1}^{tm}$are the active and the reactive power demand at the bus-$k+1$for a timetm;$V_{k+1}^{tm}$is the voltage magnitude at the bus-$k+1$for a timetm; $r_i$is the terminated line resistance to the bus-$k+1$; $N_{ln}$is the sum of lines in the network and$N_{tm}$is the overall time segments.

3.2. Bus voltage stability

Voltage stability indices are very accurate tools for measuring voltage stability of the buses through off-line. A

new voltage stability factor (VSF) is proposed in [23] for evaluating voltage stability for any bus-$k+1$at the time tm which is represented as follows

$$VSF_{k+1}^{tm} = (2V_{k+1}^{tm} - V_k^{tm}) \quad (20)$$

Average voltage stability factor per annum can be realized for a whole distribution network buses as follows

$$VSF_{a,avg} = \frac{\sum_{tm=1}^{N_{tm}} \sum_{k=2}^{N_{bs}} VSF_{k+1}^{tm}}{N_{tm}(N_{bs}-1)} \quad (21)$$

where$N_{bs}$is the total buses in the network; Bus-1 is a slack bus. The value of VSF is directly proportional to the network stability.

3.3. Network security

In a distribution network to evaluate the level of risk in the lines due to power flow network security assessment is used. Every line in a network has a certain value of transfer capacity. If these lines exceed its normal transfer capacity limits (i.e.., overloaded) then there is a chance of network congestion and creates various disturbances in the network. The ratio of power flow (MVA) through a line-$l$to its maximum line capacity (MVA) at a time$tm$is known as line loadability (LL)expressed as

$$LL_l^{tm} = \frac{L_{MVA,l}^{tm}}{L_{MVA_{max}}} \quad (22)$$

where $L_{MVA,l}^{tm}$is actual capacity and $L_{MVA_{max}}$is the line-$l$maximum capacity at the timetm.

Average network security index (NSI)per annum can be realized for a whole distribution network lines as follows [15]

$$NSI_{a,avg} = \frac{\sum_{tm=1}^{N_{tm}} \sum_{l=1}^{N_l} LL_l^{tm}}{N_{tm} * N_l} \quad (23)$$

Higher NSI value increases the risk of line outages and the lower value will consequently decrease the risk of line outages.

3.4. Constraints

The proposed method for DG planning must satisfy all equality and inequality constraints which are given as

3.4.1. Equality constraints

$$P_{ss}^{tm} + \sum_{k=2}^{N_{bs}} \sum_{j \in type} P_{DG,kj} * n_k * l_k - \sum_{k=2}^{N_{bs}} P_{D,k}^{tm} - Ploss^{tm} = 0 \quad (24)$$

$$Q_{ss}^{tm} - \sum_{k=2}^{N_{bs}} Q_{D,k}^{tm} - Qloss^{tm} = 0 \quad (25)$$

$P_{ss}^{tm}$and $Q_{ss}^{tm}$are the active and the reactive power from a substation at the timetm.$Ploss^{tm}$and $Qloss^{tm}$are the active and the reactive power loss at the timetmrespectively.

3.4.2. Inequality constraints

$$P_{DG,kj} * n_{min,k} \leq P_{DG,kj} * n_k \leq P_{DG,kj} * n_{max,k} \quad (26)$$

$n_{min,k}$and $n_{max,k}$are the minimum number and the maximum number of DGs that are connected at bus-k.

$$V_k^{tm} \leq V_{max,k} \quad (27)$$

$V_k^{tm}$is the actual voltage and $V_{max,k}$is the maximum voltage at the bus-$k$for timetm.

$$L_{MVA,l}^{tm} \leq L_{MVA_{max}} \quad (28)$$

$L_{MVA,l}^{tm}$is the actual and $L_{MVA_{max}}$is the maximum loading of line -l for timetm.

$$\sum_{k=2}^{N_{bs}} \sum_{j \in type} P_{DG,kj} * n_k * l_k \leq \sum_{k=2}^{N_{bs}} P_{D,k}^{tm} \quad (29)$$

Above constraint explains the importance of DG penetration limit. The total power generated by DG must be consumed within the distribution network. Otherwise, bidirectional power flow causes line power losses.

4. Grey Wolf Optimizer

Optimal renewable DG allocation and sizing into a distribution network is a non-linear constrained optimization problem. Various heuristic or meta-heuristic optimization techniques perform better for these type problems [14,20]. Seyedali Mirjalili et.al [21] developed grey wolf optimizer (GWO) in 2014. It is a swarm intelligence-based optimization technique which mainly employs two operators - encircling of prey (leadership hierarchy) and hunting. These are given by [21]:

4.1. Encircling of prey

In the wolf group distance between the prey and any wolf is given by

$$\vec{D} = \left| \vec{C} \otimes \vec{X}^p(t) - \vec{X}^w(t) \right| \quad (30)$$

$$\vec{C} = 2 * \vec{r}_1 \quad (31)$$

where $\vec{X}^p$ and $\vec{X}^w$is the prey and wolf position vector, and $t$indicates the iteration number. $\vec{r}_1$is a random number vector with range [0,1], and having equal dimensions of $\vec{X}^p$and $\vec{X}^w$. The symbol$\otimes$indicates component-wise multiplication between$\vec{C}$and$\vec{X}^p$.

4.2. *Hunting*

The process of approaching the prey based on the cognition in encircling is known as hunting, given by (30) and (31). This is given by

$$\vec{X}^w(t+1) = \vec{X}^p(t) - \vec{A} \otimes \vec{D} \quad (32)$$

$$\vec{A} = a * (2 * \vec{r}_2 - 1) \quad (33)$$

where$a$ is linearly reduced from 2 to 0 based on iterations, and $\vec{r}_2$ is a random number vector with range [0,1], and having equal dimensions of $\vec{X}^p$,$\vec{X}^w$and$\vec{D}$. The symbol$\otimes$indicates component-wise multiplication between $\vec{A}$and$\vec{D}$.

In the solution landscape prey position $\vec{X}^p$or the optimum solution is unknown. The wolves (α, β, and γ) [16,17] assumed here possess best knowledge about the prey. So, these three wolves' positions are applied to update the position of remaining (Omega) wolves. In decreasing order these three best solutions are arranged for fitness, the distance between the best wolves and any wolf $\vec{X}^w$is given by

$$\vec{D}_\alpha = \left|\vec{C}_1 \otimes \vec{X}^\alpha - \vec{X}^w\right|, \vec{D}_\beta = \left|\vec{C}_2 \otimes \vec{X}^\beta - \vec{X}^w\right|, \vec{D}_\gamma = \left|\vec{C}_3 \otimes \vec{X}^\gamma - \vec{X}^w\right| \quad (34)$$

The new position$\vec{X}^w(t+1)$ of the wolf can be obtained using distances as follows

$$\vec{X}_1^w = \vec{X}^\alpha - \vec{A}_1 \otimes \vec{D}_\alpha, \vec{X}_2^w = \vec{X}^\beta - \vec{A}_2 \otimes \vec{D}_\beta, \vec{X}_3^w = \vec{X}^\gamma - \vec{A}_3 \otimes \vec{D}_\gamma \quad (35)$$

$$\vec{X}^w(t+1) = \frac{\vec{X}_1^w + \vec{X}_2^w + \vec{X}_3^w}{3} \quad (36)$$

The best solution or the prey is located by applying these two operators encircling and hunting.

5. Hybrid Grey Wolf Optimizer

The performance of the GWO algorithm has been reported for benchmark functions and compared the same with other meta-heuristic algorithms like PSO, Gradient Search Algorithm (GSA), Differential Evolution (DE), Evolutionary Programming (EP) and Evolutionary Strategy (ES) in [16,17,36]. Since DG allocation is inherently discrete nature because of discrete location and size. To enhance the exploratory capability, it is suggested to hybridize GWO by adding evolutionary algorithm operators (crossover and mutation) [25].

5.1. *Crossover*

Uniform or binomial crossover [25] employed here. The j^{th}component obtained after applying crossover operator to$i^{t\square}$wolf is given by

$$X_j^i = \begin{cases} X_j^{pr} if \;\; rand_j^i < C_{pr} \\ X_j^i \;\; else \end{cases} j = 1,2,\ldots,D. \;\; i = 1,2,\ldots,N^w \quad (37)$$

where$pr \in [1,2,\ldots,N^w], r \neq i$, selected randomly, and $rand_j^i \in [0,1]$ is generated randomly$\forall \;\; j,i.D$is the solution vector dimensionality and $N^w$is the number of solutions or wolves.

Crossover rate or probability of crossover$C_{pr}$is changing dynamically for the present problem of DG allocation. This is given by [25]

$$C_{pr} = 0.2 * \hat{F}^{i,best} \quad (38)$$

$$\hat{F}^{i,best} = \frac{F^i - F^{best}}{F^{worst} - F^{best}} i = 1,2,\ldots,N^w \quad (39)$$

where $F^i$is the value ofi^{th}wolf fitness; In the wolf pack, the best fitness value is $F^{best}$and$F^{best}$is the worst fitness value for the current iteration. Equations (38) and (39) mean that for best wolf $C_{pr}$is 0 and the worst wolf it is 0.2. The best wolf vector remains unaffected. Since the probability of crossover is directly proportional to the vector.

5.2. *Mutation*

The DE mutation variant [26] employed here is classical. The j^{th}component obtained after applying mutation operator to $i^{t\square}$wolf is given by

$$x_j^i = \begin{cases} x^{gBest,j} + r_d(x_j^p - x_j^q) \;\; if \;\; rand_j^i < \mu_m \\ x_j^i \;\; else \end{cases}$$
$$i = 1,2,\ldots,D. \;\; j = 1,2,\ldots,N^w \quad (40)$$

$$\mu_m = 0.05 * \hat{F}^{i,best} \quad (41)$$

where$p,q \in [1,2,\ldots,N^w], p \neq q \neq i$, chosen randomly, and r_d, $rand_j^i \in [0,1]$ is generated randomly by mutation rate or probability of mutation isμ_m, in the entire iterative process the global best wolf j^{th}component up to current iteration is termed as $x^{gBest,j}$. In any given iteration best wolf in the pack with the global best wolf is compared. If the present best wolf is better than the global best wolf, then it turns out to be the new global best wolf. In the pack of the current iteration, equations (40) and (41) gives the best wolf,μ_m is *0* and the worst wolf it is *0.05*.

5.3. *Implementation of HGWO for optimal DG allocation*

The optimal renewable DG allocation and sizing into a distribution network reduces power losses, line loading and enhances voltage stability. In the present problem the primary control variables are DG location, size, and type. A

grey wolf (or solution vector) is formed by these set of control variables.

Evaluation of the fitness value is using equation (19) and a load flow is executed by the direct approach proposed in [27]. The grey wolves α, β, and γ are chosen in such a way that they always give the best fitness values. Based on generation output from WT and PV system and load demand-which are variables for each hour-the proposed HGWO algorithm and the load flow program is run to compute the values of power loss, VSF, and NSI as given in sections 3.1, 3.2 and 3.3 for the entire study period. The number of wolves used is 20 and the maximum number of iterations is 500. The proposed HGWO and load flow algorithms used in the present study are implemented in MATLAB® software on a personal computer with a 64-bit, 2.5 GHz, i7 processor and 8-GB RAM. The stepwise procedure to solve the optimal DG allocation problem using HGWO is as follows.

Step- 0: In the initialization step, choose the population size of the wolvesN^w, iteration number, the total number of DG locations and size to be installed. Generate the initial population of a number of grey wolves or feasible solution vector that satisfies all constraints.

$$\boldsymbol{P} = \begin{bmatrix} l_1^1, l_2^1, \dots, l_{N_{bs,k}}^1 & P_1^1, P_2^1, \dots, P_{N_{bs,k}}^1 \\ l_1^2, l_2^2, \dots, l_{N_{bs,k}}^2 & P_1^2, P_2^2, \dots, P_{N_{bs,k}}^2 \\ \vdots & \vdots \\ l_1^{N_w}, l_2^{N_w}, \dots, l_{N_{bs,k}}^{N_w} & P_1^{N_w}, P_2^{N_w}, \dots, P_{N_{bs,k}}^{N_w} \end{bmatrix} \quad (42)$$

Step- 1: Run the load flow for various values of the grey wolf and find the network power loss, VSF and NSI and the objective or fitness function (24) fitness value is evaluated. For the first iteration$p^{gBest} = p^{\alpha}$identify the wolves α, β, and γ and$p^{gBest}$the global best solution.

Step- 2: Encircle operator (34) is applied to evaluate

$$\vec{D}_{\alpha} = \left|\vec{C}_1 \otimes \vec{P}^{\alpha} - \vec{P}^{i}\right|, \vec{D}_{\beta} = \left|\vec{C}_2 \otimes \vec{P}^{\beta} - \vec{P}^{i}\right|, \vec{D}_{\gamma} = \left|\vec{C}_3 \otimes \vec{P}^{\gamma} - \vec{P}^{i}\right| \quad (43)$$

Hunting operator (35) is applied to evaluate$\vec{P}_1, \vec{P}_2$and$\vec{P}_3$,

$$\vec{P}^1 = P^{\alpha} - \vec{A}_1 \otimes \vec{D}_{\alpha}, \vec{P}^2 = P^{\beta} - \vec{A}_2 \otimes \vec{D}_{\beta}, \vec{P}^3 = P^{\gamma} - \vec{A}_3 \otimes \vec{D}_{\gamma} \quad (44)$$

Evaluate the$P(t+1)$ next generation population:

$$\vec{P}^i(t+1) = \frac{\vec{P}_1 + \vec{P}_2 + \vec{P}_3}{3}; i = 1,2,\dots,N^w \quad (45)$$

Step- 3: Apply the crossover (37) and mutation (40) operators by replacing X_j^iwithP_j^i.

Step- 4: Check for DG capacity (size) limits are violation. Check for stopping condition, if yes stop. Else repeat *steps* 1 to 3.

To compute the performance indices of the network a segment-wise generation and load model is used as shown in Fig. 1. Solar and wind PDFs are modeled and allocated in distribution system, repectively. The flow chart of proposed HGWO algorithm is as shown in Fig. 2. Sequence of steps involved in optimal allocation of solar and wind DG using HGWO is illustrated.

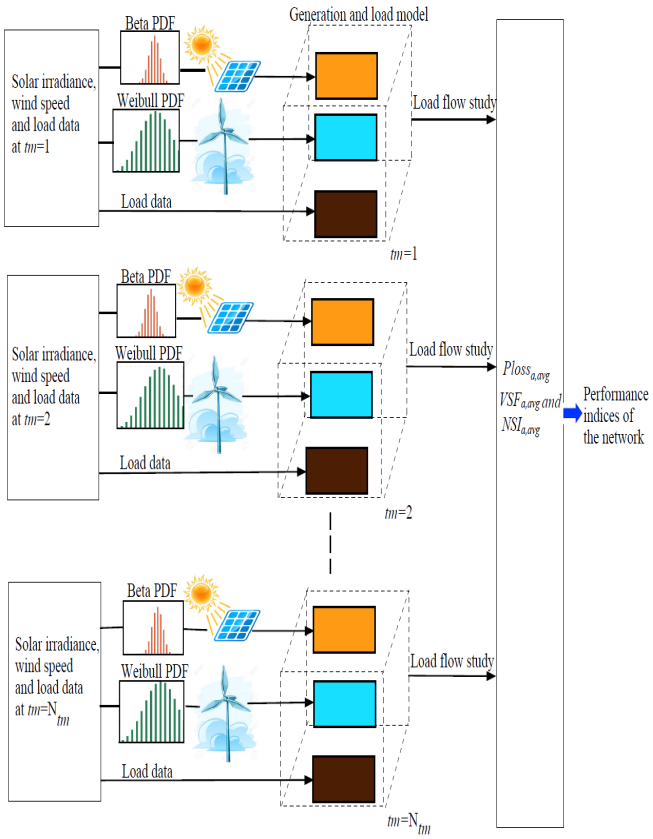

Fig. 1. Generation and load model configuration for performance evaluation.

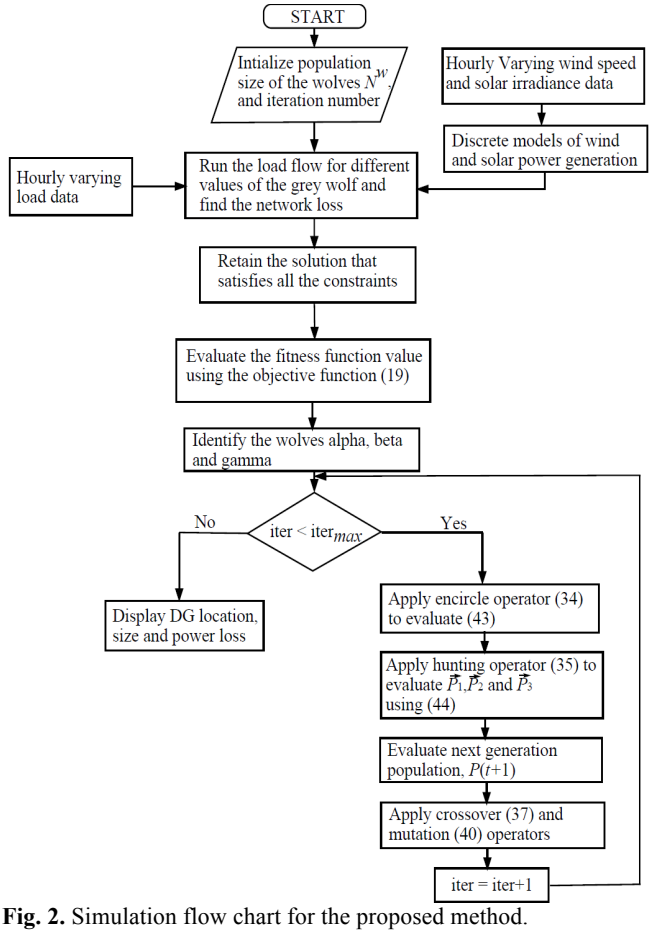

Fig. 2. Simulation flow chart for the proposed method.

6. Test System and Local Resources

The proposed HGWO algorithm was tested on 11 kV, rural 28-bus RDS located at Kakdwip province in India (21°52'N, 88°11'E). The network has a simple radial structure as shown in Fig. 3. The total peak load demand on the network is 947 kVA. However, load demand on this network is seasonally varying. Fig. 4 shows the variation in active power demand and Fig. 5 shows the variation in reactive power demand [15]. The bus, load and line loadability limit data can be obtained from [20].

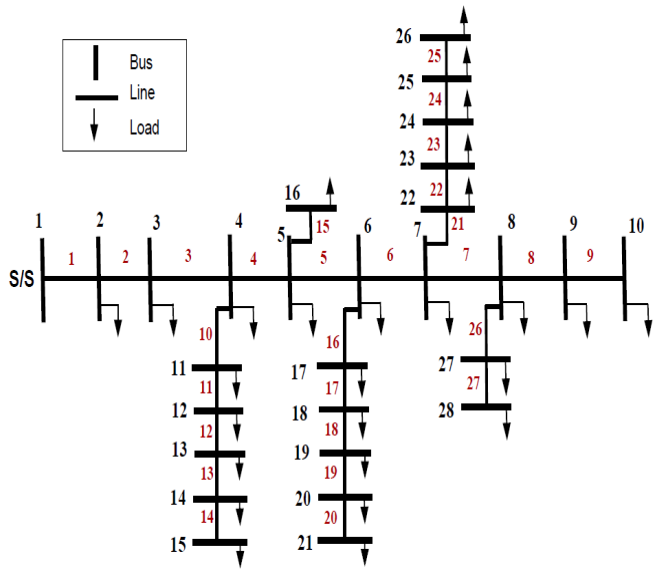

Fig. 3. A 28-bus RDS single line diagram.

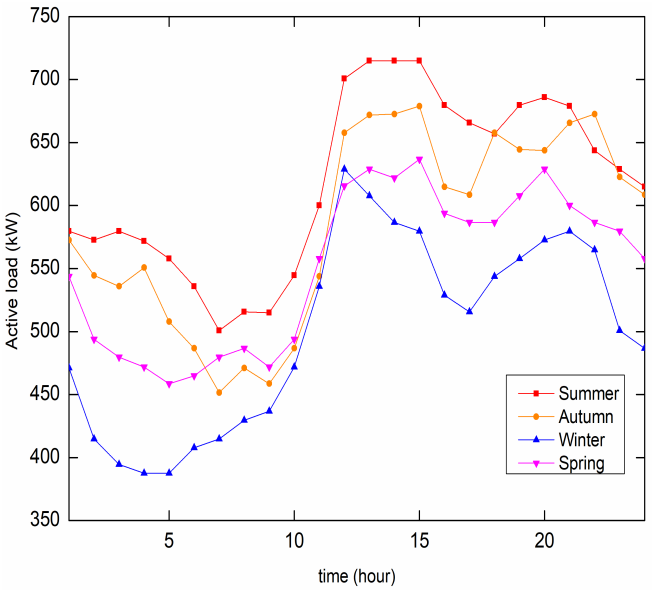

Fig. 4. Illustration of an hourly based seasonally varying active load.

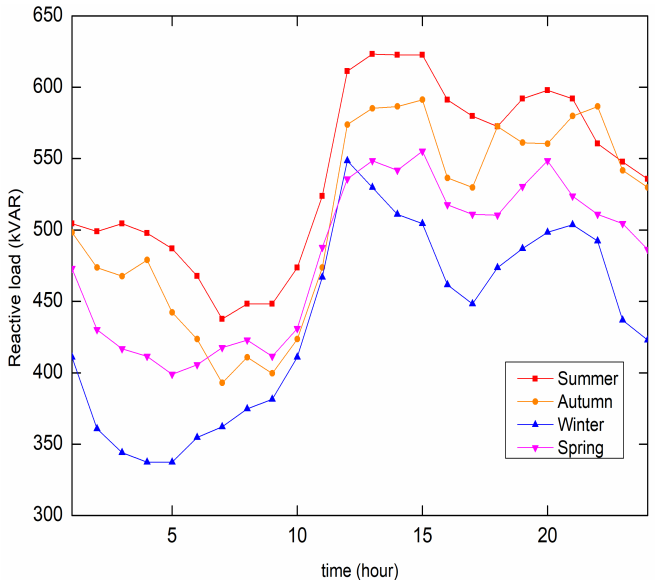

Fig. 5. Illustration of an hourly based seasonally varying reactive load.

6.1. *Resource analysis*

Kakdwip province is located near to Bay of Bengal. Due to this, it has distinct seasonal variations in weather. The study period considered here is one-year. This one-year is divided into four seasons. These seasons are summer, autumn, winter, and spring. Every season is divided here into 24 segments, in which each season has a similar hourly interval during the entire season. Thus, there are 96 segments (24 segments*4 seasons = 96segments or hours) for four seasons. In this present study 96 segments are considered as one year. Therefore, variations in network power loss, bus voltage stability, and line loading capability are shown for an annual basis. The wind speed and solar irradiance data are obtained from Ref [15]. For every hour based on historical resource data, Beta (solar irradiance) and Weibull (wind speed) PDF are generated. The number of states for Beta and Weibull PDF is 20 and 15 respectively. In spring wind speed discrete probability distribution and in summer solar irradiance is illustrated in Fig. 6 and Fig. 7 respectively.

It is assumed that at each candidate bus a maximum of three WTs or PV systems of each size can be allocated. Power generation by WT is dependent on the specification provided in Table 1 with a maximum capacity of 250 kW. A total of 600 modules are used for PV system of 132 kW installed capacity and each PV module [22] specification is given in Table 2. The predicted power generated by each of WT and PV system for the entire year is plotted in Fig. 8. It is observed that because of stochastic nature of wind speed and solar irradiance the output is varying throughout the study period.

Table 1. Specifications of wind turbine

Parameter	Quantity
Rated power (kW)	250
Cut-out speed (m/s)	25
Nominal wind speed (m/s)	12
Cut-in speed (m/s)	3

Table 2. Specifications of solar PV

Parameter	Value
Voltage at MPP, V_{MPP}	28.36 V
Current at MPP, I_{MPP}	7.76 A
Open circuit voltage, V_{oc}	36.96 V
Voltage temperature co-efficient	0.1278 V/□C
Short circuit current, I_{sc}	8.38 A
Current temperature co-efficient	0.00545 A/□C
Nominal cell operating temperature, N_{OT}	43□C

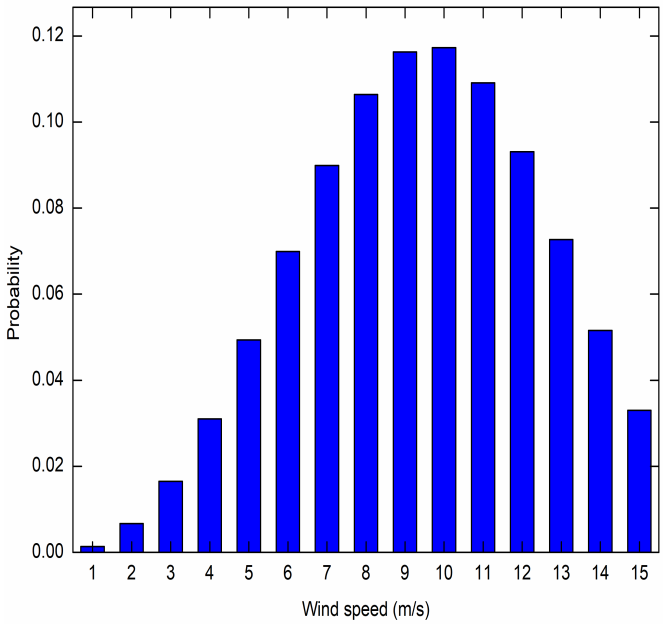

Fig. 6. Wind speed discrete probability distribution in spring.

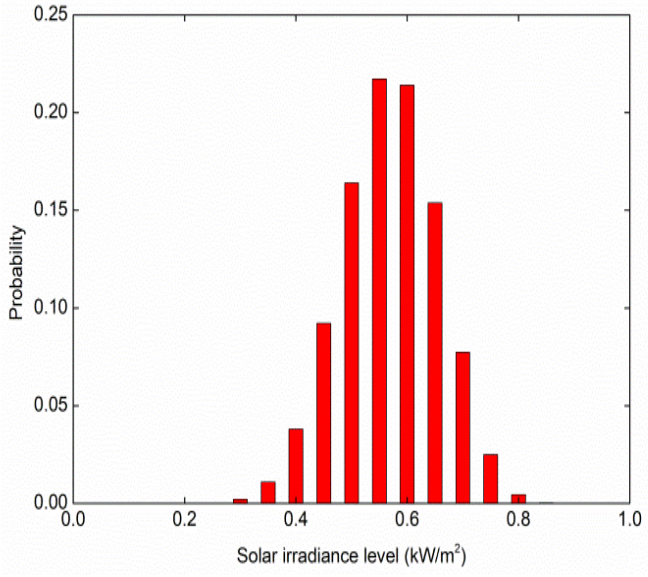

Fig. 7. Solar irradiance discrete probability distribution in summer.

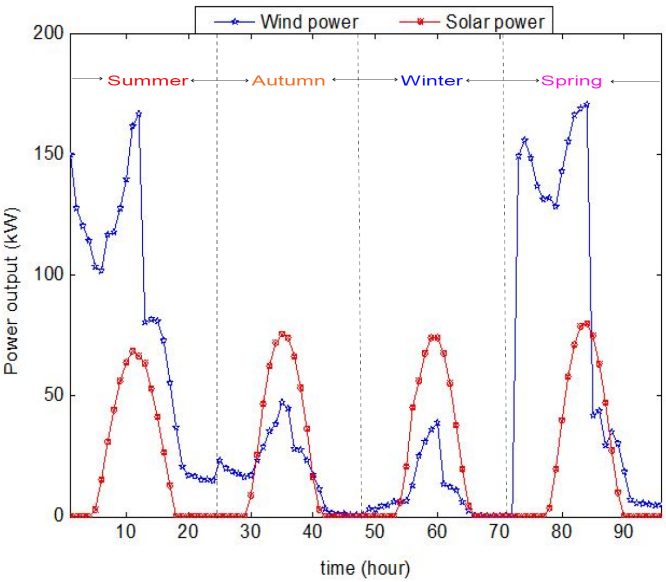

Fig. 8. Wind and solar power output during a year.

7. Results and Discussion

All buses (27-load bus) are considered for DG allocation except the slack bus. The optimum solution found by the proposed HGWO and its comparison with PSO algorithm [15] in terms of DG location, size and type are presented in Table 3. The comparison of the results obtained by the proposed HGWO algorithm with PSO for all three conditions i.e., only WT, only PV system, and mixed wind-solar system are presented in Table 4. From the Table, it is observed that significant reduction in network power loss and line loading and improvement in the bus voltage profile is achieved by the proposed HGWO algorithm. In comparison with PSO algorithm with only wind DG, there is a reduction of 37.36% in annual average power loss, improvement of 3.43% in voltage stability factor and a slight rise of 7.15% in line loading. With only solar DG, an annual average power loss reduction of 12.86% and voltage stability improvement of 0.84%, and a 2.34% decrease in line loading are achieved using the HGWO. When the network is configured with mixed wind-solar system an annual average power loss reduction of 35.5%, voltage stability improvement of 3.32% and 6.16% decrease in line loading are obtained when compared with PSO algorithm.

The DG penetration impacts on the distribution network performance seasonally with only WT, only PV system and mixed wind-solar system are shown in Fig. 9 – 17.

Fig. 9 shows the variation of the power loss without DG, and with only wind DG using HGWO. Also shown is the power loss variation with optimal DG using PSO [15], for comparison. Obviously, the power loss reduces with the addition of DG, and this reduction is higher for the HGWO-tuned-DG than for the PSO-tuned-DG, as can be seen in the figure.

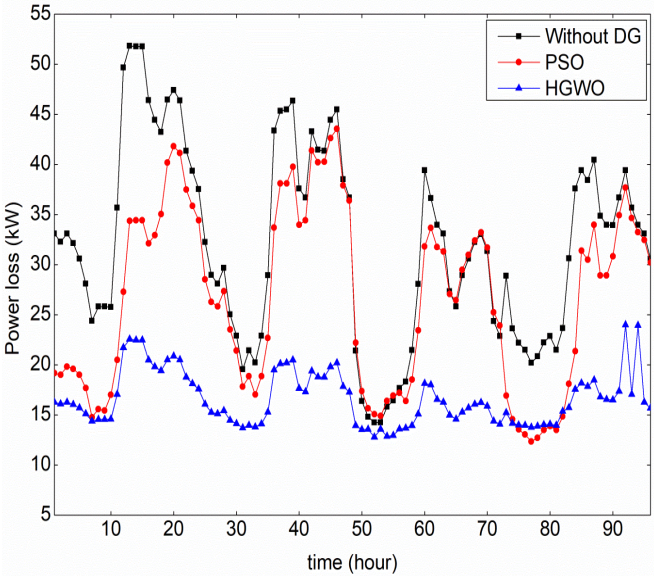

Fig. 9. Variation of power loss with only wind DG during the study period.

Fig. 10 shows the variation of the VSF without DG, and with only wind DG using HGWO. Also shown is the VSF with optimal DG using PSO [15], for comparison. Obviously, the VSF increases with the addition of DG, and this increase is higher for the HGWO-tuned-DG than for the PSO-tuned-DG, as can be seen in the figure.

Fig. 11 shows the variation of the network security index without DG, and with only wind DG using HGWO. Also shown is the network security index variation with optimal DG using PSO [15], for comparison.

Fig. 12 shows the variation of the power loss without DG, and with only solar DG using HGWO. Also shown is the power loss variation with optimal DG using PSO [15], for comparison. Obviously, the power loss reduces with the addition of DG, and this reduction is higher for the HGWO-tuned-DG, than for the PSO-tuned-DG, as can be seen in the figure.

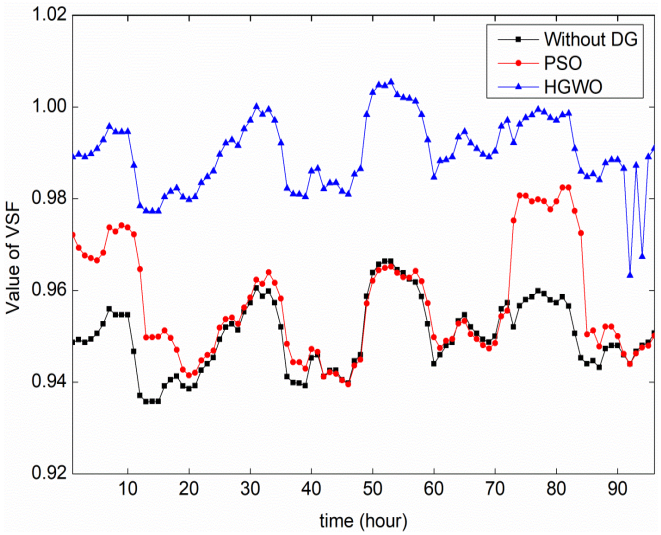

Fig. 10. Variation of network voltage stability with only wind DG during the study period.

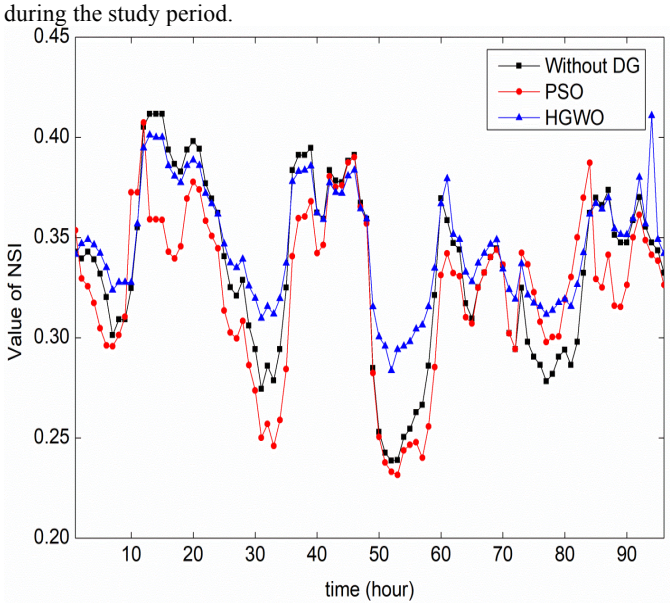

Fig. 11. Variation of network security index with only wind DG during the study period.

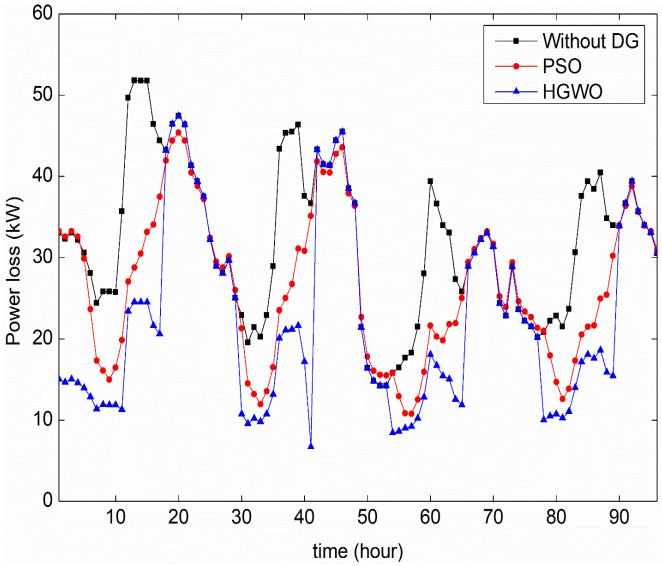

Fig. 12. Variation of power loss with only solar DG for the study period.

Table 3. Comparison of the optimum solution found by the proposed HGWO and PSO algorithm in terms of DG location, size, and type

	PSO [15]				Proposed HGWO			
Resource	Bus location	DG type	DG number	DG size	Bus location	DG type	DG number	DG size
Wind	bus-14 bus-20 bus-24	Wind	1 1 1	250 kW 250 kW 250 kW	bus-5 bus-14 bus-22	Wind	1 1 1	250 kW 250 kW 250 kW
Solar	bus-3 bus-6 bus-15 bus-24 bus-26	Solar	1 2 1 2 1	132 kW 264 kW 132 kW 264 kW 132 kW	bus-6 bus-11 bus-18	Solar	2 1 1	264 kW 132 kW 132 kW
Wind-solar	bus-9 bus-20 bus-23 bus-24	Wind Solar Solar Wind	1 1 1 1	250 kW 132 kW 132 kW 250 kW	bus-5 bus-6 bus-11 bus-18	Solar Wind Wind Solar	1 1 1 1	132 kW 250 kW 250 kW 132 kW

Table 4. Comparative study of the proposed HGWO with PSO algorithm

	Without DG	PSO [15]			Proposed HGWO		
		Wind	Solar	Wind-solar	Wind	Solar	Wind-solar

$Ploss_{a,avg}$ (kW)	32.0	26.5	26.6	26.0	**16.6**	**24.02**	**16.77**
$VSF_{a,avg}$	0.9489	0.9571	0.9570	0.9577	**0.9899**	**0.9650**	**0.9895**
$NSI_{a,avg}$	0.3344	0.3231	0.3166	0.3181	**0.3462**	**0.3121**	**0.2985**

Fig. 13 shows the variation of the VSF without DG, and with only solar DG using HGWO. Also shown is the VSF with optimal DG using PSO [15], for comparison. Obviously, the VSF increases with the addition of DG, and this increase is higher for the HGWO-tuned-DG, than for the PSO-tuned-DG, as can be seen in the figure.

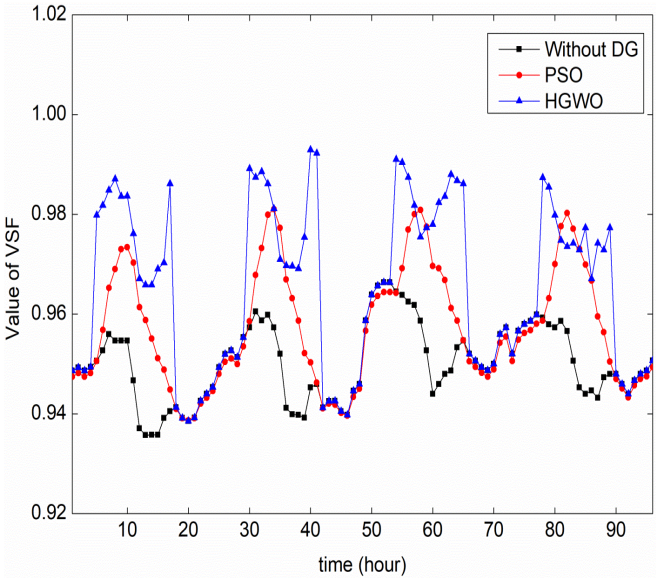

Fig. 13. Variation of network voltage stability with only solar DG during the study period.

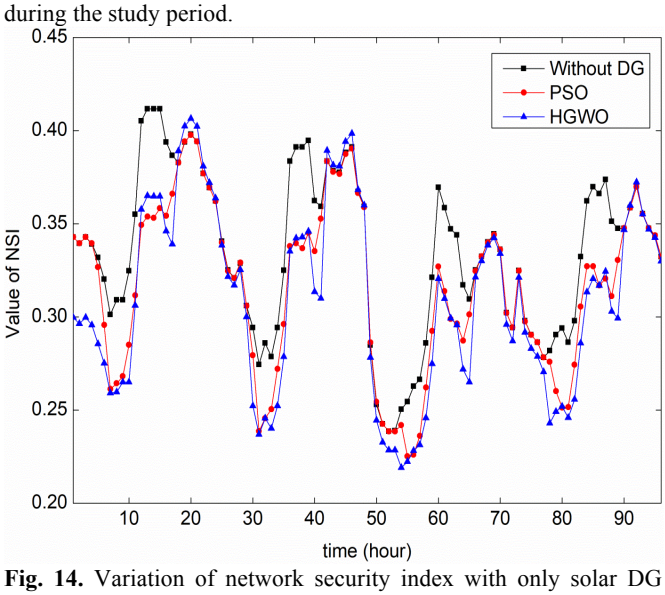

Fig. 14. Variation of network security index with only solar DG during the study period.

Fig. 14 shows the variation of the network security index without DG, and with only solar DG using HGWO. Also shown is the network security index variation with optimal DG using PSO [15], for comparison. Obviously, the NSI decreases with the addition of DG, and this decrease is higher for the HGWO-tuned-DG, than for the PSO-tuned-DG, as can be observed in the figure.

Fig. 15 shows the variation of the power loss without DG, and with mixed wind-solar DG using HGWO. Also shown is the power loss variation with optimal DG using PSO [15], for comparison. Obviously, the power loss reduces with the addition of DG, and this reduction is higher for the HGWO-tuned-DG, than for the PSO-tuned-DG, as can be seen in the figure.

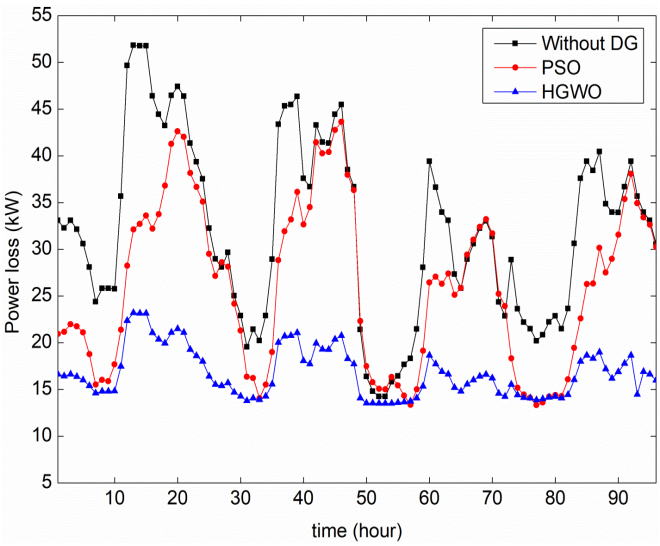

Fig. 15. Variation of power loss with mixed wind-solar DG during the study period.

Fig. 16 shows the variation of the VSF without DG, and with mixed wind-solar DG using HGWO. Also shown is the VSF with optimal DG using PSO [15], for comparison. Obviously, the VSF increases with the addition of DG, and this increase is higher for the HGWO-tuned-DG, than for the PSO-tuned-DG, as can be seen in the figure.

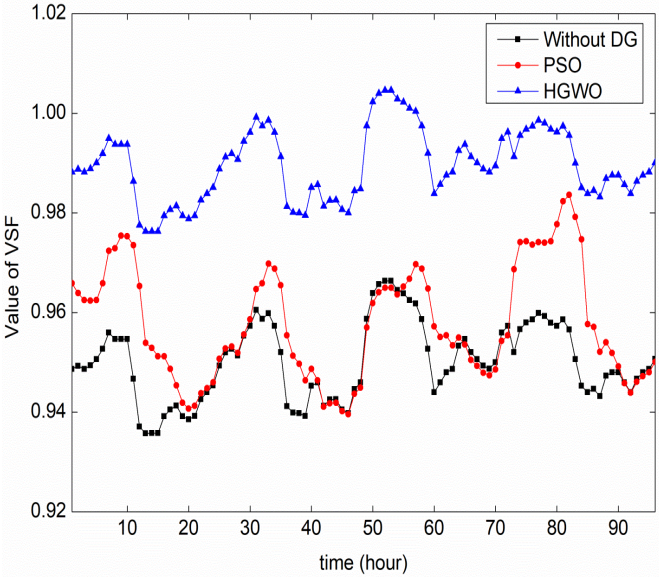

Fig. 16. Variation of network voltage stability with mixed wind-solar DG during the study period.

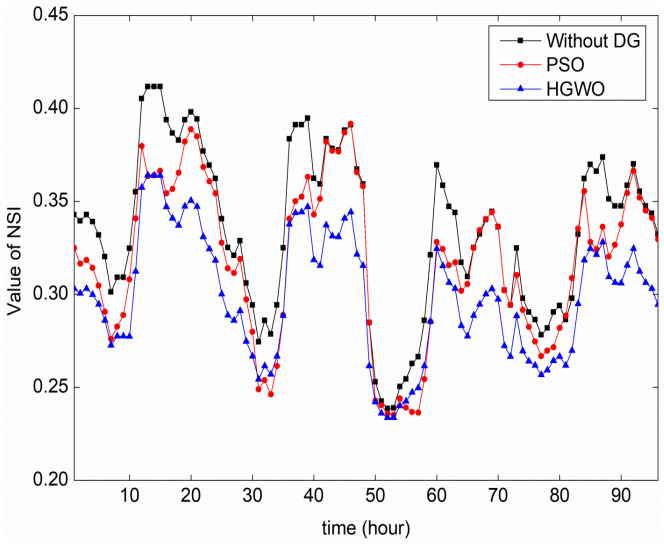

Fig. 17. Variation of network security index with mixed wind-solar DG during the study period.

Fig. 17 shows the variation of the NSI without DG, and with mixed wind-solar DG using HGWO. Also shown is the NSI variation with optimal DG using PSO [15], for comparison. Obviously, the NSI decreases with the addition of DG, and this decrease is higher for the HGWO-tuned-DG, than for the PSO-tuned-DG, as can be observed in the Fig. This behavior can be observed for the entire study period of one year. The power loss reduction by the proposed HGWO has been compared with PSO for all cases is shown in Fig. 18. From the Fig. 18 it can be observed that the proposed HGWO is performing better than PSO.

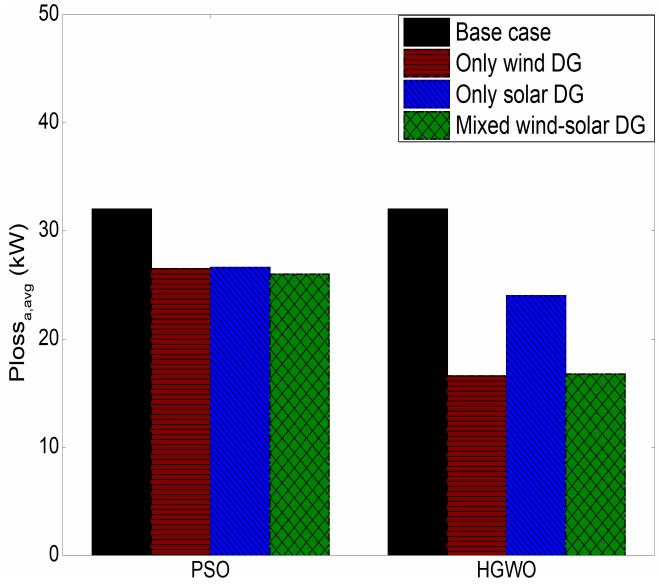

Fig. 18. Reduction in annual average power loss using the proposed HGWO compared with PSO for all cases.

8. Conclusion

A new HGWO algorithm is applied to a distribution network for solving optimal DG allocation problem in the present paper. The stochastic nature of solar and wind power generation models is developed using the probabilistic approach in which uncertainties associated with generation pattern have been modeled as PDFs. The proposed HGWO algorithm is used for network power loss minimization and evaluation of corresponding bus voltage stability index and network security index subjected to various equality and inequality constraints. The simulation results show that the HGWO algorithm performs better than the PSO algorithm in all the three cases: only wind DG, only solar DG, and mixed wind-solar DG. Optimal locations of DG with suitable size and type for entire planning period without violating any constraint are obtained. Regardless of renewable DG output pattern variations, the proposed method reduces network power loss and line loading and improves the bus voltage. Future research on the topic can include other sources of energy like fuel cells and battery storage.

Acknowledgements

The second author thanks VIT for providing 'VIT SEED GRANT' for carrying out this research work.

References

[1] Diaf S, Diaf D, Belhamel M, Haddadi M, Louche A, "A methodology for optimum sizing of autonomous hybrid PV/wind system", *Energy Policy*, vol. 35, pp. 5708-18, 2007.
[2] Ekren O, Ekren BY, "Size optimization of a PV/wind hybrid energy conversion system with battery storage using simulated annealing", *Appl Energy*, vol. 87, pp. 592-8, 2010.
[3] Zhou W, Lou C, Li Z, Lu L, Yang H, "Current status of research on optimum sizing of stand-alone hybrid solar-wind power generation systems", *Appl Energy*, vol. 87, pp. 380-9, 2010.
[4] Viral R, Khatod DK, "Optimal planning of distributed generation systems in distribution system: a review", *Renewable and Sustainable Energy Reviews*, vol. 16, pp. 5146-65, 2012.
[5] Kaabeche A, Belhamel M, Ibtiouen R, "Techno-economic valuation and optimization of integrated photovoltaic/wind energy conversion system", *Solar Energy*, vol. 85, pp. 2407-20, 2011.
[6] Abri RSA, El-Saadany EF, Atwa YM, "Optimal placement and sizing method to improve the voltage stability margin in a distribution system using distributed generation", *IEEE Trans Power Syst*, vol. 28, pp. 326-34, 2013.
[7] Ochoa LF, Padilha-Feltrin A, Harrison GP, "Evaluating distributed generation impacts with a multi-objective index", *IEEE Trans Power Del*, vol. 21, pp. 1452-8, 2006.
[8] Celik AN, "Techno-economic analysis of autonomous PV-wind hybrid energy systems using different sizing methods", *Energy Convers Manage*, vol. 44, pp. 1951-68, 2003.
[9] Yang H, Lu L, Zhou W, "A novel optimization sizing model for hybrid solar wind power generation system", *Solar Energy*, vol. 81, pp. 76-84, 2007.
[10] Sreeraj ES, Chatterjee K, Bandyopadhyay S, "Design of isolated renewable hybrid power systems", *Solar Energy*, vol. 84, pp. 1124-36, 2010.
[11] Koutroulis E, Kolokotsa D, Potirakis A, Kalaitzakis K, "Methodology for optimal sizing of stand-alone

photovoltaic/wind-generator systems using genetic algorithms", *Solar Energy*, vol. 80, pp. 1072-88, 2006.

[12] Yang H, Zhou W, Chengzhi L., "Optimal design and techno-economic analysis of a hybrid solar-wind power generation system", *Appl Energy*, vol. 86, pp. 163-9, 2009.

[13] Mikati M, Santos M, Armenta C., "Electric grid dependence on the configuration of a small-scale wind and solar power hybrid system", *Renewable Energy*, vol. 57, pp. 587-93, 2013.

[14] Khatod DK, Pant V, Sharma J, "Evolutionary programming based optimal placement of renewable distributed generators", *IEEE Trans Power Syst*, vol. 28, pp. 683-95, 2013.

[15] Kayal P, Chanda CK., "Optimal mix of solar and wind distributed generations considering performance improvement of electrical distribution network", *Renewable Energy*, vol. 75, pp. 173-86, 2015.

[16] Jayabarathi T, Raghunathan T, Adarsh BR, Nagaratnam P., "Economic dispatch using hybrid grey wolf optimizer", *Energy*, vol. 111, pp. 630-41, 2016.

[17] Sanjay R, Jayabarathi T, Raghunathan T, Ramesh V, Mithulananthan N., "Optimal allocation of distributed generation using hybrid grey wolf optimizer", *IEEE Access*, vol. 5, pp. 14807-18, 2017.

[18] Atwa YM, El-Saadany EF, Salama MMA, Seethapathy R., "Optimal renewable resources mix for distribution system energy loss minimization", *IEEE Trans Power Syst*, vol. 25, pp. 360-70, 2010.

[19] Evangelopoulos VA, Georgilakis PS., "Optimal distributed generation placement under uncertainties based on point estimate method embedded genetic algorithm", *IET Generation, Transmission & Distribution,* vol. 8, pp. 389-400, 2014.

[20] Singh RK, Goswami SK. "Multi-objective Optimization of Distributed Generation Planning Using Impact Indices and Trade-off Technique", *Electr Power Compon Syst*, vol. 39, pp. 1175-90, 2011.

[21] S. Mirjalili, S.M. Mirjalili, and A. Lewis, "Grey wolf optimizer," *Advances in Engineering Software*, vol. 69, pp. 46-61, 2014.

[22] Hung DQ, Mithulananthan N, Bansal RC., "Integrating of PV and BES units in commercial distribution systems considering energy loss and voltage stability", *Appl Energy*, vol. 113, pp. 1162-70, 2014.

[23] Kayal P, Chanda CK.," Placement of wind and solar based DGs in distribution system for power loss minimization and voltage stability improvement", *Elect Power Energy Syst*, vol. 53, pp. 795-809, 2013.

[24] Rezaei M, Moradi MH, Amini MH. "A simultaneous approach for optimal allocation of renewable energy sources and electric vehicle charging stations in smart grids based on improved GA- PSO algorithm", *Sustain Cities Soc*, vol. 32, pp. 627-37, 2017.

[25] Das S, Suganthan PN., "Differential Evolution: A Survey of the state-of-the-art", *IEEE Transactions on Evolutionary Computation* vol. 15, pp. 4-31, 2011.

[26] Hossein A, Hossein A., "Krill herd: A new bio-inspired optimization algorithm", *Commun Nonlinear Sci Numer Simul*, vol. 17, pp. 4831-45, 2012.

[27] Teng J., "A Direct Approach for Distribution System Load Flow Solutions", *IEEE Trans on Power Deli*, vol. 18, pp. 882-7, 2003.

[28] KOLA, SAMBAIAH SAMPANGI. "A Review on Optimal Allocation and Sizing Techniques for DG in Distribution Systems." International Journal of Renewable Energy Research (IJRER) 8, no. 3 (2018): 1236-1256.

[29] F. Tooryan, E. R. Collins, A. Ahmadi and S. S. Rangarajan, "Distributed generators optimal sizing and placement in a microgrid using PSO," *2017 IEEE 6th International Conference on Renewable Energy Research and Applications (ICRERA)*, San Diego, CA, 2017, pp.614-619. doi: 10.1109/ICRERA.2017.8191133.

[30] Sirine Essallah, Adel Bouallegue and Adel Khedher, "Optimal Sizing and Placement DG Units in Radial Distribution System", *International Journal of Renewable Energy Research (IJRER),* vol. 8(1), pp. 166-177, 2018.

[31] Abdelkader Harrouz, Meriem Abbes, llhami Colak, Korhan Kayisli, "Smart grid and renewable energy in Algeria", *2017 IEEE 6th International Conference on Renewable Energy Research and Applications (ICRERA)*, San Diego, CA, 2017, pp.1166-1171. doi: 10.1109/ICRERA.2017.8191237.

[32] Y. Mura, H. Minowa, Y. Nakayama, Y. Morihiro and K. Takeno, "A study of stand-alone power supply for "small green base station" with photovoltaic system," *2017 IEEE 6th International Conference on Renewable Energy Research and Applications (ICRERA)*, San Diego, CA, 2017, pp. 1172-1174. doi: 10.1109/ICRERA.2017.8191238.

[33] A. Allik and A. Annuk, "Transient processes in small scale autonomous photovoltaic and wind power systems," *2017 IEEE 6th International Conference on Renewable Energy Research and Applications (ICRERA)*, San Diego, CA, 2017, pp. 159-163. doi: 10.1109/ICRERA.2017.8191259.

[34] K. C. Wijesinghe, "Feasibility of solar PV integration in to the grid connected telecom base stations and the ultimate challenge," *2017 IEEE 6th International Conference on Renewable Energy Research and Applications (ICRERA)*, San Diego, CA, 2017, pp. 1154-1159. doi: 10.1109/ICRERA.2017.8191235.

[35] R. R. A. Galvão, R. H. A. Gonzalez, T. J. L. França and B. C. Pinheiro, "Monitoring and control system for distributed energy generation plants," *2017 IEEE 6th International Conference on Renewable Energy Research and Applications (ICRERA)*, San Diego, CA, 2017, pp. 833-838. doi: 10.1109/ICRERA.2017.8191177

[36] D. Motyka, M. Kajanová and P. Braciník, "The Impact of Embedded Generation on Distribution Grid Operation," *2018 7th International Conference on Renewable Energy Research and Applications (ICRERA)*, Paris, France, 2018, pp. 360-364. doi: 10.1109/ICRERA.2018.8566741